



# Sulfation of a squid ink polysaccharide and its inhibitory effect on tumor cell metastasis

Shiguo Chen<sup>a,1</sup>, Jingfeng Wang<sup>a,1</sup>, Changhu Xue<sup>a,\*</sup>, Hui Li<sup>a</sup>, Beibei Sun<sup>a</sup>, Yong Xue<sup>a</sup>, Wengang Chai<sup>b</sup>

<sup>a</sup> College of Food Science and Technology, Ocean University of China, 5 Yu Shan Road, Qingdao, Shandong 266003, China

<sup>b</sup> Glycosciences Laboratory, Faculty of Medicine, Imperial College London, Northwick Park and St. Mark's Campus, Harrow, Middlesex, United Kingdom

## ARTICLE INFO

### Article history:

Received 12 January 2010

Received in revised form 2 March 2010

Accepted 3 March 2010

Available online 9 March 2010

### Keywords:

Squid ink polysaccharide

Sulfation

Nuclear magnetic resonance migration

Angiogenesis

## ABSTRACT

This paper is the first to report the preparation, characterization, and potential biological activities of a chemically sulfated polysaccharide isolated from the ink of the squid, *Ommastrephes bartrami*. The squid ink polysaccharides (SIPs) were firstly sulfated with the pyridine–sulfur-trioxide complex in dimethyl sulfoxide. Structural characterization of sulfated SIP using nuclear magnetic resonance indicated that sulfation mainly occurred at the 4,6-position of GalNAc. The effects of the sulfated SIP (TBA-1) on tumor cell growth, invasion, and migration were examined in vitro, and its effects on angiogenesis were measured in vivo using the chick embryo chorioallantoic membrane (CAM) assay. TBA-1 did not have any obvious effects on the proliferation of HepG2 tumor cells, but induced the dose-dependent suppression of cell invasion and migration in HepG2. Moreover, TBA-1 obviously inhibited angiogenesis in a CAM model. Thus, our results indicate that TBA-1 is a potential candidate compound for the prevention of tumor metastasis.

Crown Copyright © 2010 Published by Elsevier Ltd. All rights reserved.

## 1. Introduction

Sulfated polysaccharides, which are widespread in nature, play an important role in molecular recognition, cell development and differentiation, and cell–cell interaction. A number of natural sulfated polysaccharides were reported to exhibit diverse biological activities, such as anticoagulant activity (Athukorala, Jung, Vasanthan, & Jeon, 2006; Mourao et al., 2001; Pushpamali et al., 2008), antiviral activity (Kanekiyo et al., 2005; Lee et al., 2006; Rusnati et al., 2009), and antitumor activity (Peng, Zhang, Zeng, & Kennedy, 2005; Tong et al., 2009; Zhang, Cui, Cheung, & Wang, 2007); thus, chemical sulfation of many natural polysaccharides has been conducted. The sulfation of polysaccharides could not only enhance water solubility but also change the chain conformation, resulting in alteration of their biological activities (Chaidedgumjorn et al., 2002; Liu & Wang, 2007). New pharmacological agents with possible therapeutic uses can be obtained by chemical sulfation of polysaccharides.

A sulfated GAG-like polysaccharide has been identified in squid ink and has been reported to have antibacterial (Funatsu, Fukami, Kondo, & Watabe, 2005; Sadok, Abdelmoulah, & El Abed, 2004), antitumor (Sasaki, Ishita, Takaya, Uchisawa, & Matsue, 1997;

Takaya et al., 1994), and anti-retroviral activities (Rajaganapathi, Thyagarajan, & Edward, 2000). Several active components, including a tyrosinase and an angiotensin-converting enzyme inhibitor, have been identified (Kim, Kim, & Song, 2003; Naraoka et al., 2003; Russo et al., 2003). In our previous work (Chen et al., 2008), we isolated a non-sulfated glycosaminoglycan-like polysaccharide from melanin-free ink of the squid, *Ommastrephes bartrami*. Using electrospray ionization tandem mass spectrometry (ESI/MS/MS) and nuclear magnetic resonance (NMR) analyses, we found that its structure was composed of the following unique repeating trisaccharide:  $[-3\text{Glc}\alpha 1-4(\text{GalNAc}\alpha 1-3)\text{Fuc}\alpha 1]_n-$ . However, sulfation of this unique polysaccharide has not been reported. In this study, the squid ink polysaccharide (SIP) sulfated with pyridine–sulfur-trioxide complex in dimethyl sulfoxide (DMSO), and investigated the structures of sulfated polysaccharides by high-performance liquid chromatography (HPLC), infrared (IR), and NMR spectroscopy. We examined the effects of sulfated polysaccharides on tumor cell metastasis.

## 2. Experimental protocol

### 2.1. Materials

The ink of the squid, *O. bartrami*, was obtained from Zhou-Shan Fishery Company (Zhejiang, China) and stored at  $-40^\circ\text{C}$  before use. TSK G4000PWXL columns were obtained from TOSOH BIOSEP (Tokyo, Japan), and Sephacryl S-300, from Amersham Biosciences

\* Corresponding author.

E-mail address: [xuech@ouc.edu.cn](mailto:xuech@ouc.edu.cn) (C. Xue).

<sup>1</sup> These two authors contributed equally to this article.

(Uppsala, Sweden). The monosaccharides D-mannose (Man) and L-fucose (Fuc), papain, and cystein (Cys) were purchased from Fluka (Seelze, Germany), while L-arabinose (Ara), D-galactose (Gal), D-galactosamine (GalN), D-glucosamine (GlcN), D-glucuronic acid (GlcA), D-galacturonic acid (GalA), disaccharide lactose, trimethylamine (TMA), DMSO, tributylammonium, and pyridine–sulfur-trioxide from Sigma (St. Louis, MO, USA). The derivatization reagent 1-phenyl-3-methyl-5-pyrazolone (PMP) was purchased from Sinopharm Chemical Reagent (Shanghai, China). The RPMI-1640 medium and newborn/fetal bovine serum were obtained from Gibco Co. (USA). L-Glutamine and 3-(4,5-dimethylthiazol-2-yl)-2,5-diphenyltetrazolium bromide (MTT) were purchased from Sigma Chemical (St. Louis, MO, USA). Matrigel was obtained from BD (San Jose, CA, USA). Fertilized chicken eggs were purchased from Qingdao Zhengda Co. Ltd.

## 2.2. Isolation and purification of non-sulfated SIP

SIP was purified as previously reported (Chen et al., 2008). Briefly, melanin-free ink was digested with 2 volumes of 1% (w/v) papain in Tris–HCl buffer (50 mM (pH 6.8) containing 5 mM Cys and 5 mM EDTA) at 60 °C for 24 h. Digestion was repeated twice. Crude melanin-free SIP was obtained after precipitation with 4 volumes of ethanol. The crude SIP was purified by sequential gel filtration and anion-exchange chromatography on a Sephacryl S-300 column (1.6 cm × 100 cm) and a DEAE ion-exchange column (2.6 cm × 30 cm), respectively. The molecular weight of SIP was determined by liquid chromatography on an Agilent 1100 system (Palo Alto, CA, USA) with a TSK G4000PWXL column (TOSOH BIOSEP) by elution with 0.2 M NaCl, and it was found to be 48000 Da.

## 2.3. Sulfation of SIP

**Method 1:** The sulfation reaction was performed as follows: The polysaccharide powder (1 g) was suspended in dry DMSO (50 ml), and the mixture was stirred at 80 °C for 30 min, after which 4 g Py-SO<sub>3</sub> was added. The reaction was allowed to continue for 1–3 h; then, the mixture was cooled to room temperature with an ice bath, neutralized with 15% NaOH aqueous solution, and dialyzed against distilled water (Spectra/Por membrane, MWCO. 1000) for 120 h. The dialysate was freeze-dried and weighed. About 1.2–1.5 g of each of the sulfated SIP samples prepared with different reaction times was obtained; depending on the reaction time, they were named DMSO-1h, DMSO-2h, and DMSO-3h.

**Method 2:** SIP (1.5 g) was dissolved in water (25 ml) and passed through an ion-exchange column (50 ml, Amberlite IR-120 H1). After its passage through the column, the pH of the solution was 3.35. The pH was then adjusted to 7 with tributylamine and stirred for 1 h. Excess tributylamine was removed by extracting the resulting solution with diethyl ether. The solution was dialyzed (Spectra/Por membrane, MWCO. 1000) against water for 12 h to completely remove any remaining tributylamine (Falshaw et al., 2000). The retentate was concentrated on a rotary evaporator and finally lyophilized to obtain the tributylammonium salt of SIP (1.65 g).

The tributylammonium (TBA) salt of the SIP (1 g) was dissolved in dry DMSO (20 ml). The pyridine–sulfur-trioxide complex (15 equivalents [10 g] or 7 equivalents [5 g]) was dissolved in dry DMSO (40 ml). Both DMSO solutions were cooled on an ice bath, and the pyridine–sulfur-trioxide solution was poured into the SIP solution. The resulting solution was stirred on an ice bath for 1–3 h. After this, the mixture was poured into ice-cold water (200 ml), and the pH (initially 2) was adjusted to 7 with NaOH (2 M). The solution was dialyzed (Spectra/Por membrane, MWCO. 1000) against distilled water for 48 h and then lyophilized to obtain sulfated SIP. About 1.2–1.5 g of the sulfated SIP samples prepared with different reac-

tion times was used; depending on the reaction time, they were named TBA-1, TBA-2, and TBA-3.

## 2.4. Chemical composition of chemically modified SIP

As previously reported, the GalNAc branch is likely to be lost in acidic conditions. The monosaccharide composition of chemically modified SIP was determined by a PMP-HPLC method (Strydom, 1994). In brief, polysaccharide (typically 1 mg) was hydrolyzed with 2 M TFA at 110 °C under nitrogen for 8 h with lactose added as an internal standard. The monosaccharide hydrolysate was dried under vacuum and then derivatized with 450 µL PMP solution (0.5 M in methanol) and 450 µL of 0.3 M NaOH at 70 °C for 30 min. The reaction was discontinued by neutralization with 450 µL of 0.3 M HCl and extraction with chloroform (1 mL, 3 times). HPLC analyses were performed on an Agilent ZORBAX Eclipse XDB-C18 column (5 µm, 4.6 mm × 150 mm) at 25 °C with detection at UV (250 nm). The mobile phase was 0.05 M KH<sub>2</sub>PO<sub>4</sub> (pH 6.9) with 15% (solvent A) and 40% (solvent B) acetonitrile in water. The solvent B gradient used was from 8% to 19% for 25 min.

The sulfate content was determined by ion chromatography (Ohira & Toda, 2006).

## 2.5. NMR spectroscopy and IR spectroscopy

For NMR analysis, chemically sulfated SIP or native polysaccharide (50 mg) were co-evaporated with D<sub>2</sub>O (99.8%) twice by lyophilization before final dissolution in 500 µL high-quality D<sub>2</sub>O (99.96%) containing 0.1 µL acetone. <sup>1</sup>H NMR experiments were carried out at 600 MHz, and <sup>13</sup>C NMR experiments, at 150 MHz. The spectra for both were recorded at 60 °C for the native polysaccharide. The temperatures were selected so as to assign the HDO signals with minimal disturbance to carbohydrate protons. The observed <sup>1</sup>H chemical shifts were reported relative to internal acetone (2.03 ppm).

The IR spectrum of the polysaccharide (~0.5 mg) was acquired on a Perkin-Elmer instrument as KBr pellets at room temperature.

## 2.6. Cell line and cell culture

The human hepatocellular liver carcinoma cell line HepG2 was obtained from Shanghai Cell Bank (Shanghai, China) and grown in RPMI 1640 medium supplemented with 10% newborn bovine serum, 2 mM L-glutamine, 100 units/mL penicillin, and 100 µg/mL streptomycin at 37 °C in a humidified atmosphere containing 5% CO<sub>2</sub>. All the experiments were repeated 3 times to ensure reproducibility. The sulfated SIP TBA-1 was used for all the cell culture experiments. It was dissolved in D-Hanks as a stocking solution and diluted with the culture medium to the desired concentrations before use.

## 2.7. Cell proliferation assay

HepG2 (2 × 10<sup>4</sup> cells/well) cells were plated on a 96-well plate (Corning, NY, USA). After the cells were incubated overnight, the medium in each well was replaced by fresh RPMI1640 medium containing different concentrations of TBA-1. After incubation for 48–96 h, the medium was removed from each well, and cell viability was determined by the MTT assay, as described previously.

## 2.8. Wound migration assay

The HepG2 cells were plated in a 24-well plate and incubated for 24 h. The confluent monolayer was starved with serum-free medium for 8 h, wounded by scratching with a 1-ml pipette tip, and washed 3 times with phosphate-buffered saline (PBS). Then,

the cells were incubated in serum-free medium containing various concentrations of TBA-1. Photographs were taken at 0, 12, and 24 h after wounding, and the width of the wound was measured with the Image Pro Plus 5 software.

### 2.9. Cell invasion assay

Cell invasion assay was performed using the transwell Boyden chamber with a 6.5-mm diameter polycarbonate filter (pore size, 8  $\mu$ M). Briefly, the upper surface of each filter was coated with a uniform layer of Matrigel (diluted in RPMI-1640, 1:20, v/v). HepG2 cells were trypsinized and suspended at a final concentration of  $5 \times 10^5$  cells/mL in RPMI1640 containing 1% fetal bovine serum (FBS), and 100  $\mu$ L of the cell suspension was loaded into each upper well, along with various concentrations of TBA-1. In the lower chamber, RPMI-1640 medium containing 20% FBS was used to stimulate migration. After incubation at 37 °C for 24 h, nonmigrating cells on the upper surface of the filter were removed with a cotton swab. Migrating cells on the lower surface of the filters were fixed with ethanol and stained with 1% crystal violet. The cells were visualized using a microscope (IX70; Olympus, Japan) equipped with a 40 $\times$  objective. Five random fields were counted for each filter, and the images were analyzed using the Image Pro Plus 5 software. Each assay was performed in triplicate.

### 2.10. Chicken chorioallantoic membrane assay

Inhibition of angiogenesis was determined using a modification of the chicken chorioallantoic membrane (CAM) assay (Tan et al., 2001). Fertilized chicken eggs were transferred to an egg incubator maintained at 37 °C and 50% humidity and allowed to grow for 9 days. Then, a 1-cm<sup>2</sup> window was created. The shell membrane was removed to expose the CAM. Filter paper disks (diameter, 5 mm) saturated with TBA-1 solutions (20 and 40  $\mu$ g/egg) or PBS were placed on the CAM. The window was resealed with plastic tape, and the embryos were further incubated for 24 h. The neovascular zones under the disks were photographed using a stereomicroscope (SZ61; Olympus, Japan).

### 2.11. Statistical analysis

All data are presented as mean (SD). Statistical significance was determined by one-way analysis of variance (ANOVA) and the least significant difference (LSD) test.

## 3. Results and discussion

### 3.1. Effects of various reaction conditions on the degree of sulfation

The sulfate group plays an important role in the bioactivities of polysaccharides. The degree of sulfation (DS) of polysaccharides is an important parameter for analyzing the bioactivities. Three sulfated samples of SIP that were prepared with method 1 were named DMSO-1, DMSO-2, and DMSO-3, the DSs of which were determined to be in the range of 2.51–2.73. The molecular weight of native SIP was 48000 Da, but that of DMSO-1, DMSO-2, and DMSO-3 decreased sharply to 6000–10000 Da; this indicates that backbone degradation probably occurred because of the highly reactive environment. The sulfated samples of SIP prepared by method 2 were named TBA-1, TBA-2, and TBA-3, the DS of which were determined to be 2.13–2.25; thus, these DS values were slightly lower than those of the sulfated samples prepared using method 1. However, the molecular weight of these samples was almost unchanged compared to native SIP (molecular weight, about 30000 Da); thus, the backbone remained almost unchanged.

**Table 1**

Composition and molecular weights analysis of the sulfated SIP sample.

Samples	Molar ratio of monosaccharides						Sulfate	MW (Da)
	Fuc	GlcN	GlcA	GalN	Gal	Man		
SIP	1.00	0.14	0.96	1.01	0.03	0.08	0	48000
DMSO-1	1.00	0.11	0.74	0.84	0.03	0.15	2.41	10200
DMSO-2	1.00	0.10	0.76	0.81	–	0.17	2.63	8300
DMSO-3	1.00	0.10	0.79	0.84	–	0.13	2.75	6700
TBA-1	1.00	0.09	0.81	0.93	–	0.16	2.13	32400
TBA-2	1.00	0.08	0.80	0.92	–	0.13	2.20	31300
TBA-3	1.00	0.09	0.84	0.93	–	0.12	2.25	29800

Although the sulfation resulted in a decrease in the molecular weight, the monosaccharide composition of all 6 sulfated samples remained almost unchanged (Table 1); this indicated that the sulfation process obviously has no effect on the loss of GalNAc branches, which we have reported are liable to be lost under acidic conditions. Since there were no obvious effects of time on the chemical properties of the sulfated sample, we chose DMSO-1 and TBA-1 for further spectral analyses.

Compared with the FTIR spectrum of native SIP, that of sulfated SIP (DMSO-1 and TBA-1) showed 2 new absorption bands—one at 1248 cm<sup>−1</sup>, describing an asymmetrical S–O stretching vibration, and the other at 827 cm<sup>−1</sup>, representing a symmetrical C–O–S vibration associated with a C–O–SO<sub>3</sub> group (Fig. 1). These observations indicated the presence of 4,6-O-SO<sub>3</sub>-GalNAc or 2-O-SO<sub>3</sub>-Fuc (Bernardi & Springer, 1962; Duarte, Cardoso, Nosedá, & Cerezo, 2001).

### 3.2. NMR spectrum characterization of sulfated SIP

The <sup>1</sup>H NMR spectrum of the SIP is shown in Fig. 2(a): 3 narrow doublet peaks were observed at 5.27 ppm (d, *J* = 3.42), 5.18 ppm (d, *J* = 3.64), and 4.52 ppm (d, *J* = 6.06); they were attributed to the anomeric protons of Fuc ( $\alpha$ ), GalNAc ( $\alpha$ ), and GlcA ( $\beta$ ), respectively. However, the splits of the sulfated sample were obviously unclear, and a new major signal around the anomeric region at 5.56 ppm appeared; this was assigned to the anomeric signal of 4,6-sulfated GalNAc ( $\alpha$ ) according to previous reports. Moreover, a minor signal at 5.86 ppm could not be assigned; this might be the 2, 4, 6-O-sulfated group of branch GalNAc ( $\alpha$ ). The anomeric protons of Fuc ( $\alpha$ ) shift from 5.27 ppm (d, *J* = 3.42) to 4.98 ppm; this shift was caused by sulfation of GalNAc.

The <sup>13</sup>C NMR spectrum further confirmed the results of the <sup>1</sup>H NMR spectrum (Fig. 3). The resonance peaks at 173–176 ppm in

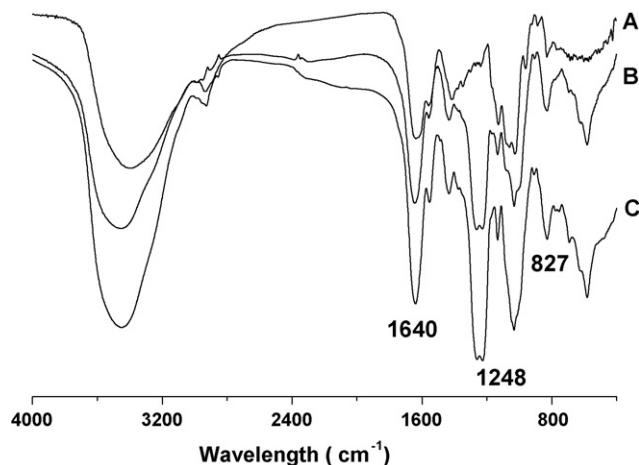


**Fig. 1.** IR spectrum of squid ink polysaccharides and its sulfated derivatives. (a) Native SIP; (b) DMSO-1; (c) TBA-1.

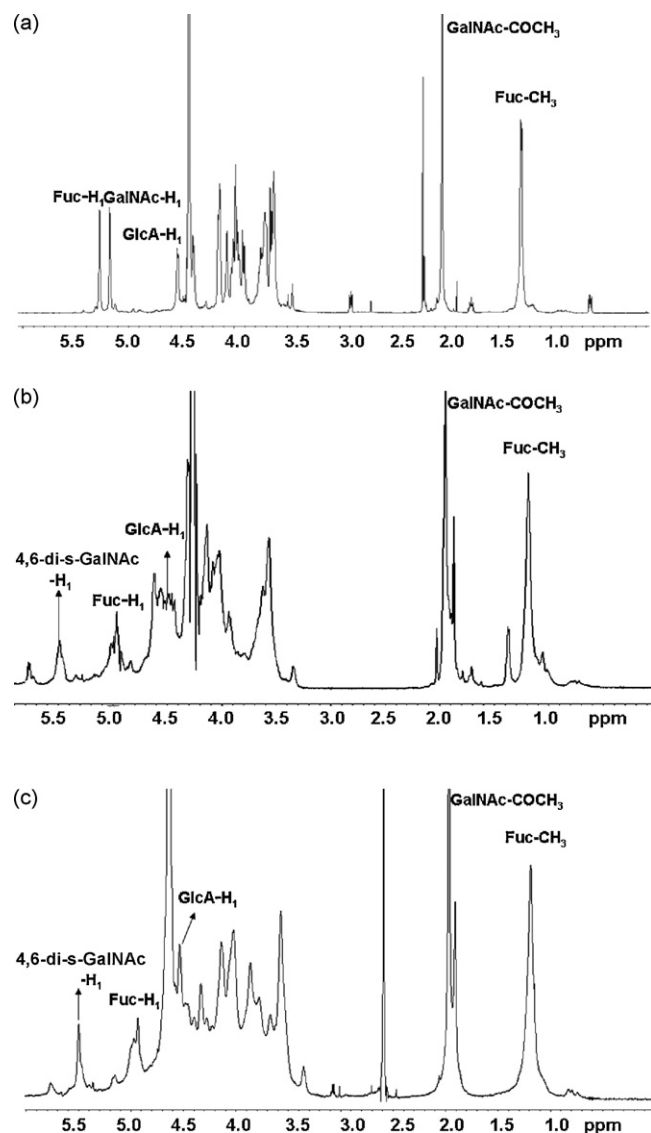


Fig. 2.  $^1\text{H}$  NMR of squid ink polysaccharides and its sulfated derivatives. (a) Native SIP; (b) DMSO-1; (c) TBA-1.

the  $^{13}\text{C}$  NMR spectra of all the samples were assigned to the carbonyl group of GlcA and GalNAc. The main signal of GalNAc in SIP was assigned to 101.87 ppm for C1, 74.1 ppm for C5, 71.3 ppm for C4, 70.1 ppm for C3, 52.4 ppm for C2, and 64.5 ppm for C6. The peak at 64.5 ppm, which represented the chemical shift of C6 of GalNAc in native SIP, disappeared in the  $^{13}\text{C}$  NMR spectrum of TBA-1 and DMSO-1. The new peak that appeared at 68.5 ppm indicated the sulfation of C6 in the GalNAc of TBA-1 and DMSO-1 because the downfield shift of a carbon atom linked by a sulfated group is 4–7 ppm. Similarly, the new peaks at 77.9 ppm for TBA-1 and DMSO-1 were assigned to the substituted C4 of GalNAc, which were fully substituted by sulfate groups. Furthermore, a new peak at 100.3 ppm was assigned to C1 of GalNAc, because C4 and C6 had been substituted by sulfate group to influence the chemical shift of the adjacent C1. In DMSO-1, the anomeric signal of GalNAc splits into 2 peaks—100.3 ppm for C1 and 99.5 ppm for C1'. The upfield shift of C1' to C1 is 0.8 ppm, indicating that the C2, C4, and C6 of partial GalNAc are substituted by sulfate, which is in line with Gorin's description.

All the results indicated that sulfation mainly occurred at the 4,6-position of GalNAc. The main structure of the sulfated SIP should be  $-\left[3\text{GlcA}\beta 1-4(4,6\text{-SO}_4\text{-GalNAc}\alpha 1-3)\text{Fuc}\alpha 1\right]_n-$ .

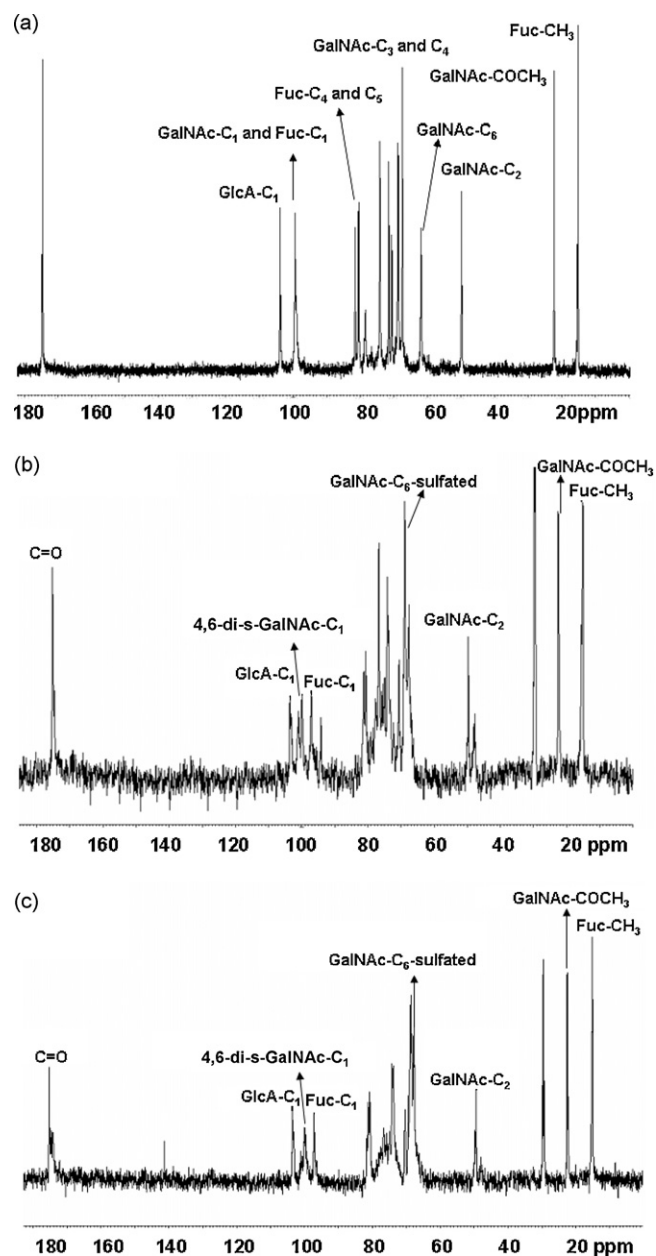
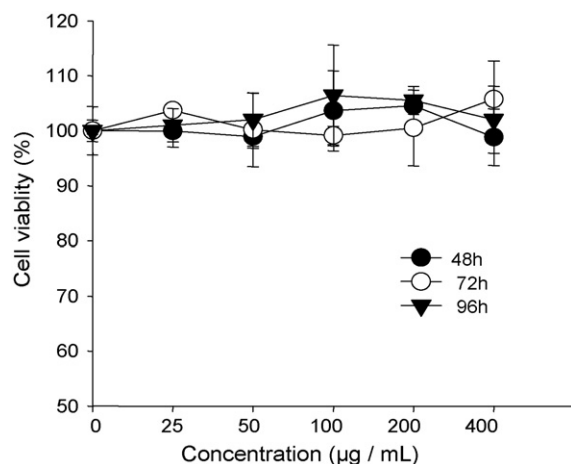


Fig. 3.  $^{13}\text{C}$  NMR of squid ink polysaccharides and its sulfated derivatives. (a) Native SIP; (b) DMSO-1; (c) TBA-1.

### 3.3. Anti-metastasis activity of chemically sulfated SIP

To identify the effect of TBA-1 on anti-metastasis, we initially examined the effects of TBA-1 on tumor cell proliferation by the MTT assay. Data indicated that TBA-1 at the tested concentrations did not inhibit HepG2 proliferation (Fig. 4). To investigate whether TBA-1 inhibits tumor migration, wound migration assays were performed in TBA-1-treated HepG2 cells. As shown in Fig. 5, TBA-1 suppressed the migration of HepG2 across the wounded space in a dose-dependant manner. Tumor cell migration and invasion are necessary for metastasis. We further explored the effect of TBA-1 on HepG2 invasion by using a transwell Boyden chamber assay. Incubation of control HepG2 for 24 h resulted in large-scale invasion of tumor cells to the lower side of the filter (Fig. 6). In contrast, treatment with TBA-1 inhibited HepG2 invasion in a dose-dependent manner, resulting in inhibition rates of 38.4% and 78.2%. Invasion is a characteristic feature of carcinomas, which frequently show





**Fig. 4.** Effects of TBA-1 on HepG2 cell proliferation. Cells were cultured in the presence of TBA-1 (25–400 µg/ml) for 48–96 h and the cell growth was measured using MTT assay. Data are mean  $\pm$  SD ( $n = 3$ ).

early invasion into blood vessels and subsequent tumor metastasis (Pasco, Brassart, Ramont, Maquart, & Monboisse, 2005). These results suggest that the sulfated SIP TBA-1 may be useful for suppressing HepG2 cell metastasis. Furthermore, TBA-1 had no obvious cytotoxic effects on HepG2, indicating that inhibition of HepG2 cell metastasis by TBA-1 is likely to occur in a cytotoxicity-independent fashion.

The CAM of the chicken embryo is a unique model for evaluating neovascularization. Using this model, we examined the potential anti-angiogenic activities of TBA-1 in vivo. In the control eggs, blood vessels formed densely branching vascular networks (Fig. 7). Treatment with TBA-1 significantly inhibited the number of newly formed blood vessels in a dose-dependent manner; this suggests that TBA-1 suppresses angiogenesis in chicken embryos.

Angiogenesis, the process of the sprouting of new capillaries from pre-existing blood vessels, is essential for sustained growth of solid tumors and metastasis (Folkman, 2002). The sulfated polysaccharide SIP-SII from the ink of the cuttlefish, *Sepiella maindroni*, might suppress invasion and migration of carcinoma cells via inhibition of MMP-2 proteolytic activity; these polysaccharides are composed of fucose, *N*-acetylgalactosamine, and mannose in a

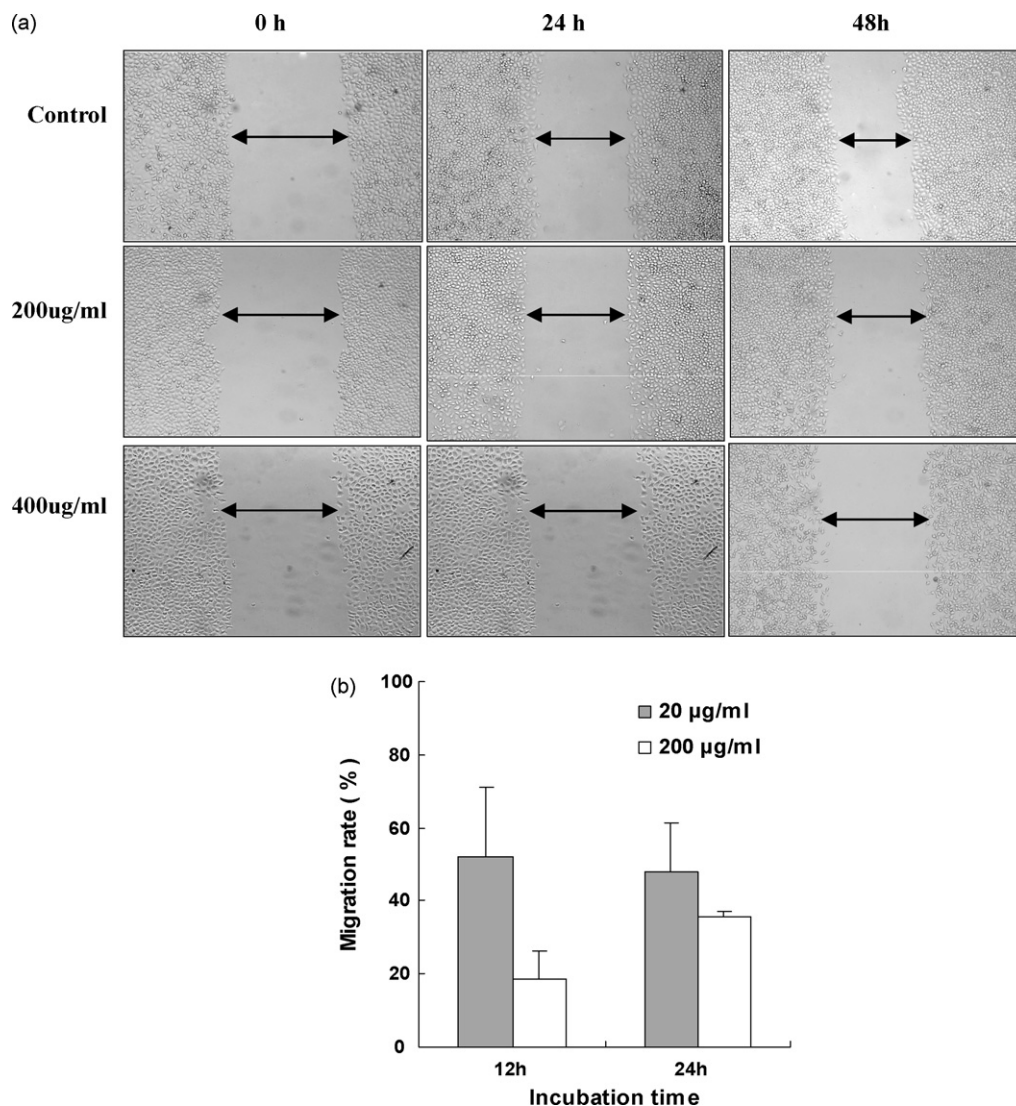


**Fig. 5.** Inhibition of HepG-2 cell migration by TBA-1. The cells were plated in a 24-well plate and confluent monolayer were wounded and then incubated in serum-free medium in 200 and 400 µg/mL of TBA-1. At 0, 12 and 24 h after wounding, the cells were photographed under an invert microscope and width of the migration was measured. Microphotographs of HepG2 cells (a) and quantitative analysis (b) of the wound migration assay are shown. Migration rate was expressed as a percentage of control (0 µM).

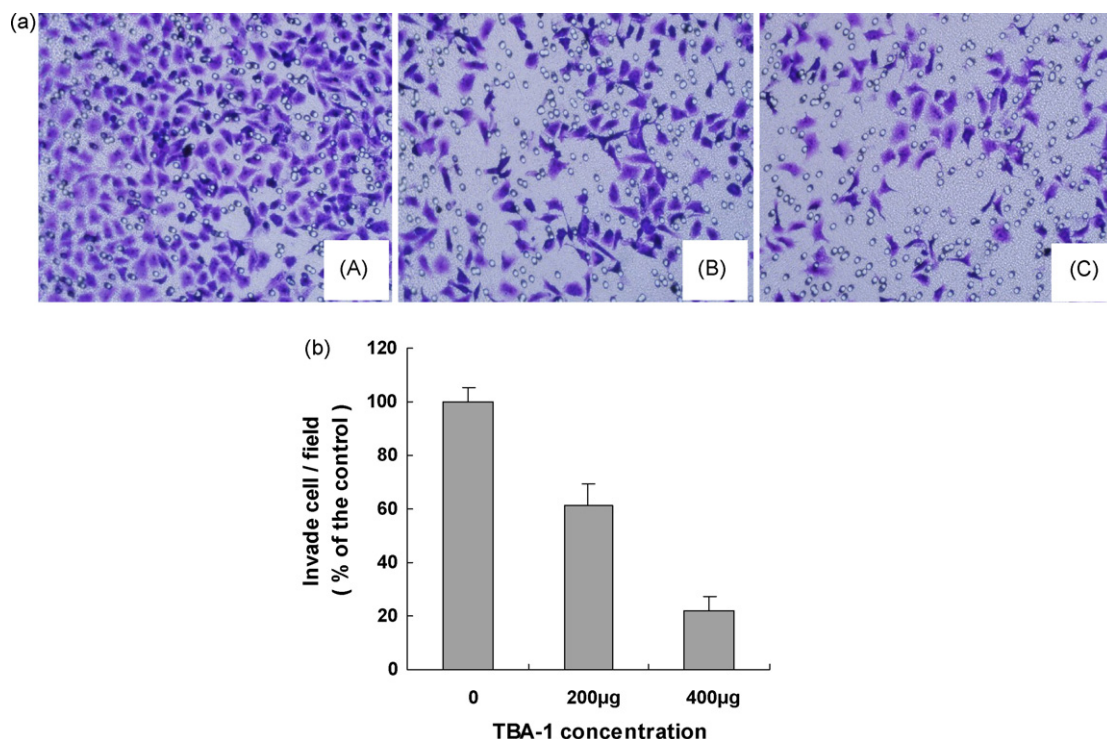


**Fig. 6.** Inhibition of HepG-2 cell invasion by TBA-1. (a) Cells pre-treated with various concentrations of TBA-1 were placed on Matrigel-coated filters and incubated for 24 h. Invasion cells on the lower surface of the filter were assessed by staining with crystal violet. (A) Control; (B) 200 µg/ml; (C) 400 µg/ml. (b) Overall rate of TBA-1-induced inhibition of HepG-2 migration.

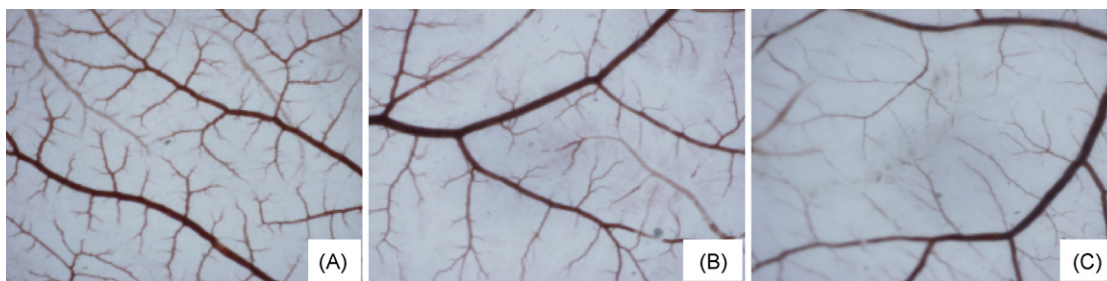


**Fig. 7.** The effects of TBA-1 on the angiogenesis of CAM. Fertilized eggs were incubated continuously for 9 days, and then a window was opened to expose the CAM and DSEA was added to a final concentration of (A) 0 µg/egg (PBS control), (B) 20 µg/egg, (C) 40 µg/egg. The eggs were incubated for another 24 h, and then the treated CAMs were harvested and photographed by stereoscope (Olympus SZ61, Japan).

molar ratio of 2:2:1, with a single branch of glucuronic acid at the C-3 position of mannose (Wang et al., 2008). Here, we show that sulfated SIPs have anti-metastatic activity. However, the detailed mechanism still requires further investigation.

#### 4. Conclusion

An SIP with the clear unique structure  $-\text{[3Glc}\alpha\text{1-4(GalNAc}\alpha\text{1-3)-Fuc}\alpha\text{1]}_n-$  was first sulfated with the pyridine-sulfur-trioxide complex in DMSO; no obvious degradation of SIP occurred. Two characteristic absorption bands (near 1258 and 827  $\text{cm}^{-1}$ ) appeared in the FT-IR spectra, which indicated that the sulfation reaction had actually occurred. Further,  $^1\text{H}$  and  $^{13}\text{C}$  NMR spectra indicated that sulfation mainly occurred at the 4,6-position of GalNAc. The main structure of the sulfated SIP was clearly shown to be  $-\text{[3Glc}\alpha\text{1-4(4,6-SO}_4\text{-GalNAc}\alpha\text{1-3)-Fuc}\alpha\text{1]}_n-$ . We further investigated the effects of the sulfated SIP TBA-1 on invasion and migration of tumor cells in vitro and on angiogenesis in vivo. Our findings are the first to provide evidence for the inhibition of tumor cell invasion and suppression of angiogenesis by the unique

sulfated SIP TBA-1. These results suggest that TBA-1 may be a candidate compound for the prevention of tumor metastasis.

#### Acknowledgements

This work was supported by the National High-tech Research and Development Project of China (Nos. 2006AA09Z444 and 2007AA091802), National Natural Science Foundation of China (Nos. 30871944 and 30972284). We thank Xiuli Zhang (Ocean University of China) for NMR experiments.

#### References

- Athukorala, Y., Jung, W., Vasanthan, T., & Jeon, Y. (2006). An anticoagulative polysaccharide from an enzymatic hydrolysate of *Ecklonia cava*. *Carbohydrate Polymers*, 66(2), 184–191.
- Bernardi, G., & Springer, G. (1962). Properties of highly purified fucan. *Journal of Biological Chemistry*, 237(1), 75–80.
- Chaidedgumjorn, A., Toyoda, H., Woo, E., Lee, K., Kim, Y., Toida, T., et al. (2002). Effect of (1 → 3)- and (1 → 4)-linkages of fully sulfated polysaccharides on their anticoagulant activity. *Carbohydrate Research*, 337(10), 925–933.
- Chen, S., Xu, J., Xue, C., Dong, P., Sheng, W., Yu, G., et al. (2008). Sequence determination of a non-sulfated glycosaminoglycan-like polysaccharide from

- melanin-free ink of the squid *Ommastrephes bartrami* by negative-ion electrospray tandem mass spectrometry and NMR spectroscopy. *Glycoconjugate Journal*, 25(5), 481–492.
- Duarte, M., Cardoso, M., Nosedá, M., & Cerezo, A. (2001). Structural studies on fucoidans from the brown seaweed *Sargassum stenophyllum*. *Carbohydrate Research*, 333(4), 281–293.
- Falshaw, R., Hubl, U., Ofman, D., Slim, G., Amjad Tariq, M., Watt, D., et al. (2000). Comparison of the glycosaminoglycans isolated from the skin and head cartilage of Gould's arrow squid (*Nototodarus gouldi*). *Carbohydrate Polymers*, 41(4), 357–364.
- Folkman, J. (2002). *Role of angiogenesis in tumor growth and metastasis*. Elsevier., pp. 15–18.
- Funatsu, Y., Fukami, K., Kondo, H., & Watabe, S. (2005). Improvement of "kurozukuri ika-shiokara" (fermented squid meat with ink) odor with *Staphylococcus nepalensis* isolated from the fish sauce mush of frigate mackerel *Auxis rochei*. *Bulletin of the Japanese Society of Scientific Fisheries*, 71, 611–617.
- Kaneakiyo, K., Lee, J., Hayashi, K., Takenaka, H., Hayakawa, Y., Endo, S., et al. (2005). Isolation of an antiviral polysaccharide, nostoflan, from a terrestrial cyanobacterium, *Nostoc flagelliforme*. *Journal of Nature Products*, 68(7), 1037–1041.
- Kim, S., Kim, S., & Song, K. (2003). Partial purification and characterization of an angiotensin-converting enzyme inhibitor from squid ink. *Agricultural Chemistry and biotechnology*, 46, 9–13.
- Lee, J., Hayashi, K., Hirata, M., Kuroda, E., Suzuki, E., Kubo, Y., et al. (2006). Antiviral sulfated polysaccharide from *Navicula directa*, a diatom collected from deep-sea water in Toyama Bay. *Biological & Pharmaceutical Bulletin*, 29(10), 2135–2139.
- Liu, Y., & Wang, F. (2007). Structural characterization of an active polysaccharide from *Phellinus ribis*. *Carbohydrate Polymers*, 70(4), 386–392.
- Mourao, P. A., Boisson-Vidal, C., Tapon-Brethaudiere, J., Drouet, B., Bros, A., & Fischer, A. (2001). Inactivation of thrombin by a fucosylated chondroitin sulfate from echinoderm. *Thrombosis Research*, 102(2), 167–176.
- Naraoka, T., Uchisawa, H., Mori, H., Matsue, H., Chiba, S., & Kimura, A. (2003). Purification, characterization and molecular cloning of tyrosinase from the cephalopod mollusk, *Illex argentinus*. *European Journal of Biochemistry*, 270(19), 4026.
- Ohira, S., & Toda, K. (2006). Ion chromatographic measurement of sulfide, methanethiolate, sulfite and sulfate in aqueous and air samples. *Journal of Chromatography A*, 1121(2), 280–284.
- Pasco, S., Brassart, B., Ramont, L., Maquart, F., & Monboisse, J. (2005). Control of melanoma cell invasion by type IV collagen. *Cancer Detection and Prevention*, 29(3), 260–266.
- Peng, Y., Zhang, L., Zeng, F., & Kennedy, J. (2005). Structure and antitumor activities of the water-soluble polysaccharides from *Ganoderma tsugae* mycelium. *Carbohydrate Polymers*, 59(3), 385–392.
- Pushpamali, W., Nikapitiya, C., Zoysa, M., Whang, I., Kim, S., & Lee, J. (2008). Isolation and purification of an anticoagulant from fermented red seaweed *Lomentaria catenata*. *Carbohydrate Polymers*, 73(2), 274–279.
- Rajaganapathi, J., Thyagarajan, S., & Edward, J. (2000). Study on cephalopod's ink for anti-retroviral activity. *Indian Journal of Experimental Biology*, 38(5), 519.
- Rusnati, M., Vicenzi, E., Donalisio, M., Oreste, P., Landolfo, S., & Lembo, D. (2009). Sulfated K5 *Escherichia coli* polysaccharide derivatives: A novel class of candidate antiviral microbicides. *Pharmacology and Therapeutics*, 123(3), 310–322.
- Russo, G., De Nisco, E., Fiore, G., Di Donato, P., d'Ischia, M., & Palumbo, A. (2003). Toxicity of melanin-free ink of *Sepia officinalis* to transformed cell lines: Identification of the active factor as tyrosinase. *Biochemical and Biophysical Research Communications*, 308(2), 293–299.
- Sadok, S., Abdelmoula, A., & El Abed, A. (2004). Combined effect of sepia soaking and temperature on the shelf life of peeled shrimp *Penaeus kerathurus*. *Food Chemistry*, 88(1), 115–122.
- Sasaki, J., Ishita, K., Takaya, Y., Uchisawa, H., & Matsue, H. (1997). Anti-tumor activity of squid ink. *Journal of Nutritional Science and Vitaminology*, 43, 455–461.
- Strydom, D. (1994). Chromatographic separation of 1-phenyl-3-methyl-5-pyrazolone-derivatized neutral, acidic and basic aldoses. *Journal of Chromatography A*, 678(1), 17–23.
- Takaya, Y., Uchisawa, H., Matsue, H., OKUZAKI, B., Narumi, F., Sasaki, J., et al. (1994). An investigation of the antitumor peptidoglycan fraction from squid ink. *Biological & Pharmaceutical Bulletin*, 17(6), 846–849.
- Tan, D., Kini, R., Jois, S., Lim, D., Xin, L., & Ge, R. (2001). A small peptide derived from Flt-1 (VEGFR-1) functions as an angiogenic inhibitor. *FEBS Letters*, 494(3), 150–156.
- Tong, H., Xia, F., Feng, K., Sun, G., Gao, X., Sun, L., et al. (2009). Short communication: Structural characterization and in vitro antitumor activity of a novel polysaccharide isolated from the fruiting bodies of *Pleurotus ostreatus*. *Bioresource Technology*, 100(4), 1682–1686.
- Wang, S., Cheng, Y., Wang, F., Sun, L., Liu, C., Chen, G., et al. (2008). Inhibition activity of sulfated polysaccharide of *Sepiella maindroni* ink on matrix metalloproteinase (MMP)-2. *Biomedicine & Pharmacotherapy*, 62, 297–302.
- Zhang, M., Cui, S., Cheung, P., & Wang, Q. (2007). Antitumor polysaccharides from mushrooms: A review on their isolation process, structural characteristics and antitumor activity. *Trends in Food Science & Technology*, 18(1), 4–19.